

# Optimum design of damped vibration absorber for viscoelastic bladed disk assemblies

Amir Abdollah Ghaderi\*, Alireza Mohammadzadeh\*\*, Mansour Nikkhah Bahrami\*\*\*

\*Department of Mechanical and Aerospace Engineering, Science and Research Branch, Islamic Azad University, Tehran, Iran, E-mail: a.a.ghaderi@gmail.com

\*\*Department of Mechanical and Aerospace Engineering, Science and Research Branch, Islamic Azad University, Tehran, Iran, E-mail: a-mohamadzadeh@srbiau.ac.ir

\*\*\*Department of Mechanical and Aerospace Engineering, Science and Research Branch, Islamic Azad University, Tehran, Iran, E-mail: m-nikkhah@srbiau.ac.ir

crossref <http://dx.doi.org/10.5755/j01.mech.21.6.13243>

## 1. Introduction

High cycle fatigue is known as the main cause of failure of rotating structures such as compressor blades, pumps and so on. Many researchers have determined blade as the most critical component of those structures [1-8]. Blade vibrations are examined under various conditions and methods are provided to suppress vibration especially in resonant conditions [1,9-17]. The goal of this investigation is to study the effectiveness of blades equipped with optimum damped order tuned vibration absorber for vibration suppression of rotationally periodic bladed disk assemblies. Effect of mistuning are omitted and therefor system is considered with fully cyclic symmetry. During steady operation, these systems rotate at a constant speed and are subjected to engine order excitation which is a traveling wave dynamic loading type and proportional to the mean rotational speed of the rotor. Disk is supposed as being rigid. To represent the viscoelastic behaviour of blades, Kelvin-Voigt model is chosen. Lumped parameters of a model with one degree of freedom are extracted for the blades. Inter-blade coupling (due to the shrouds, aerodynamic damping and etc.) is considered. Each of the blades, are fitted with a damped order-tuned vibration absorber. With comparison between the behaviours of the elastic blades with the viscoelastic blades, which are used for first time in this investigation, the effects of viscosity of the material have been ignored. The optimum values of the absorber parameters, includes mass, damping and length of the pendulum of the absorber, are determined for both viscoelastic and elastic blades by using numerical method and  $H_2$  optimization criterion. The objective of optimization criterion is to reduce the total vibration energy of the system over all frequency, so the area (called  $H_2$  norm) under frequency response curve of the system is minimized [18].

## 2. Formulation

Because of omitting the mistuning effects, an idealized perfectly tuned model of system, which contains of a cyclic chain of  $N$  identical, identically coupled blades that are uniformly attached to a rigid disk, is considered. Each blade is modelled as Euler-Bernoulli cantilever beam with constant material property and thickness. To represent the linear viscoelastic behaviour of the beam, Kelvin-Voigt model is chosen.

Transverse vibration of the beams is studied. According to Eq. (1) which introduces the relationship between the bending moment ( $M(x,t)$ ) and deflected shape ( $w(x,t)$ ) of the beam, equivalent flexural stiffness and damping constant of the beam is extracted:

$$P(M(x,t)) = -I \left( \frac{\partial^2 w(x,t)}{\partial x^2} \right). \quad (1)$$

$P$  and  $Q$  are introduced as below:

$$P = \sum_{k=0}^m P_k \frac{d^k}{dt^k} \quad \text{and} \quad Q = \sum_{k=0}^m Q_k \frac{d^k}{dt^k}. \quad (2)$$

Because of the harmonic characterization of applied load and according to Equation. (3) which is the complex compliance for Kelvin-Voigt model for the linear viscoelastic behaviour of materials:

$$J^*(\omega) = \frac{1}{E + \mu_v i \omega}. \quad (3)$$

And due to the boundary conditions of the beam, after some analytical simplification, equivalent flexural stiffness and damping constant of viscoelastic beam is extracted as below:

$$K_e = \frac{3EI_b}{L^3} \quad \text{and} \quad C_e = \frac{3\mu_v I_b}{L^3}. \quad (4)$$

In the Eq. (4),  $K_e$  and  $C_e$  are the equal viscoelastic stiffness and damping parameters,  $E$  is the elastic modulus and  $\mu_v$  is the viscosity of the material,  $\omega$  is the angular frequency,  $L$  is the length of the beam (effective length of the blade) and  $I_b$  is its moment of inertia. In this paper, the model with one degree of freedom is considered for each blade. According to Fig. 1 the provided model is included  $N$  pendulums with the lengths of  $L_a$  and the lumped masses of  $M_a$  that are uniformly attached to the periphery of a rigid disk with a radius of  $H$ . The disk rotates with the constant speed of  $\Omega$  around the axis through A [15].

With using Eq. (4), the flexural viscoelastic stiffness and damping of each blades are modeled with a linear

torsional springs and dampers in the attachment point of the blade to the disk. Inter-blade coupling (due to the shrouds, aerodynamic damping and etc.) is modeled in the distances of  $r_a$  and with linear springs and dampers [15].

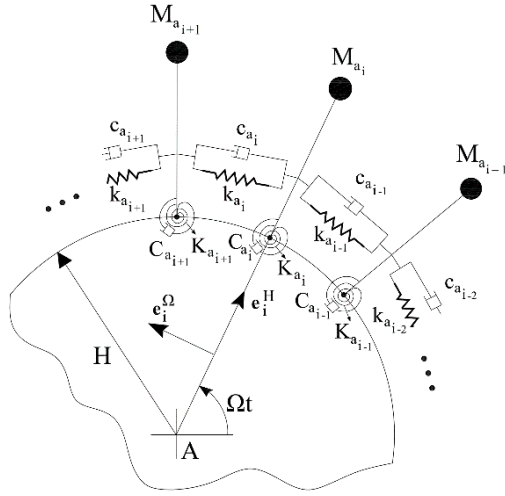


Fig. 1 Lumped parameter model of flexible rotating blades [15]

The blade angle is shown with  $\theta_{a_i}$ . For purely radial configuration of the blades, it is assumed that the springs and dampers are unstressed. Effect of rotational inertia is ignored and identical absorber that is modeled by a simple pendulum with the length of  $d_b$  and mass of  $m_a$  are fitted in the each of the blades.

Damping of absorber is modelled using a torsional damper acts at attachment point of absorber pendulum to the blade (point P).  $\beta_b$  describes the angle of absorber which is relative to its corresponding blade.

The terms related to blade and absorber is introduced in Table 1.

Table 1

List of variables and parameters of blade and absorber

Parameter	Description	Unit
$\Omega$	Angular speed	Rad/s
$H$	Radius of the disk	m
$L_a$	Length of the blade	m
$d_b$	Length of the absorber	m
$r_a$	Distance from base point of blade to inter-coupling elements attachment point	m
$M$	Blade total mass	Kg
$M_a$	Blade lumped mass	Kg
$m_a$	Absorber mass	Kg
$K$	Blade stiffness	N/m
$K_a$	Blade lumped stiffness	N/m
$k_a$	Stiffness coupling between sectors	N/m
$C_a$	Blade lumped damping	N.s/m
$c_a$	Damping coupling between sectors	N.s/m
$C_b$	Absorber damping	N.s/m

Fig. 2 shows the blade and the absorber fitted in it, which is constituted the sector [15].

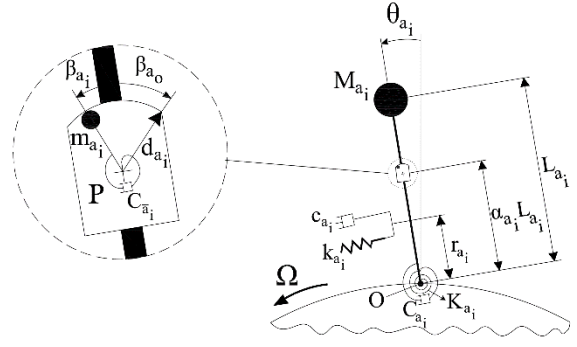


Fig. 2 Sector model of flexible rotating blades [15]

The kinetic energy of the entire system is extracted according to Eq. (5)

$$\begin{aligned}
 T_i = & \sum \frac{1}{2} M_{a_i} \left( H^2 \Omega^2 + L_{a_i}^2 (\Omega + \dot{\theta}_{a_i})^2 + \right. \\
 & + 2H\Omega L_{a_i} (\Omega + \dot{\theta}_{a_i}) \cos(\theta_{a_i}) \left. + \right. \\
 & + \frac{1}{2} m_{a_i} \left( H^2 \Omega^2 + \alpha_{a_i}^2 L_{a_i}^2 (\Omega + \dot{\theta}_{a_i})^2 + \right. \\
 & + d_{a_i}^2 (\Omega + \dot{\theta}_{a_i} + \dot{\beta}_{a_i})^2 + \\
 & + 2\alpha_{a_i} L_{a_i} H \Omega (\Omega + \dot{\theta}_{a_i}) \cos(\theta_{a_i}) + \\
 & + 2H\Omega d_{a_i} (\Omega + \dot{\theta}_{a_i} + \dot{\beta}_{a_i}) \cos(\theta_{a_i} + \beta_{a_i}) + \\
 & \left. + 2\alpha_{a_i} L_{a_i} d_{a_i} (\Omega + \dot{\theta}_{a_i}) (\Omega + \dot{\theta}_{a_i} + \dot{\beta}_{a_i}) \cos(\beta_{a_i}) \right). \quad (5)
 \end{aligned}$$

Gravitational effects are ignored and due to the elastic inter-blade coupling and flexural stiffness of the blades, the system potential energy is given by Eq. (6)

$$\begin{aligned}
 V = & \sum \frac{1}{2} K_{a_i} \theta_{a_i}^2 + \frac{1}{2} k_{a_i} r_{a_i}^2 (\theta_{a_{i+1}} - \theta_{a_i})^2 + \\
 & + \frac{1}{2} k_{a_{i-1}} r_{a_{i-1}}^2 (\theta_{a_i} - \theta_{a_{i-1}})^2. \quad (6)
 \end{aligned}$$

According to Eq. (7), the Rayleigh dissipation function describes the damping of the absorber and the inter-blade damping:

$$\begin{aligned}
 R = & \sum \frac{1}{2} C_{a_i} \dot{\theta}_{a_i}^2 + \frac{1}{2} c_{a_i} r_{a_i}^2 (\dot{\theta}_{a_{i+1}} - \dot{\theta}_{a_i})^2 + \\
 & + \frac{1}{2} c_{a_{i-1}} r_{a_{i-1}}^2 (\dot{\theta}_{a_i} - \dot{\theta}_{a_{i-1}})^2 + \frac{1}{2} C_{b_i} \dot{\beta}_{a_i}^2. \quad (7)
 \end{aligned}$$

The blades are forced harmonically and in the transverse sense by engine order excitation of order  $n$ . The range of  $0 < n < N$  is considered for the excitation order. The values of  $n \geq N$ , will not affect the results [15]. The engine order excitation is modeled with the Eq. (8):

$$Q_i^{(\theta_{a_i})} = F_o L_{a_i} e^{j\phi_i} e^{jn\Omega t} \quad \text{and} \quad Q_i^{(\beta_{a_i})} = 0. \quad (8)$$

In the above equation,  $F_o$  is strength of excitation and  $\phi_i = 2\pi \frac{n}{N} (i-1)$  is inter-blade phase angle [15]. La-

grange's method is employed and the equations of motion are extracted. To extract the dimension-less form of the equations, the time is rescaled according to  $\tau = \omega_o t$  and

$\omega_o = \sqrt{\frac{K}{ML^2}}$  is the undamped natural frequency of single isolated blade. Next, the dimension-less form of the equations are extracted according to the parameters that are defined in Table 2 and are linearized for small blades and absorbers motions.

In matrix-vector form, equations of motion for the 2DOF sector (blade with the absorber) are given by Eq. (9):

$$Mz_i'' + Cz_i' + Kz_i + C_c(-z_{i-1}' + 2z_i' - z_{i+1}') + K_c(-z_{i-1} + 2z_i - z_{i+1}) = fe^{j\phi_i} e^{jn\sigma t}, i \in N. \quad (9)$$

Table 2  
Descriptions and values of dimensionless variables and parameters

Parameter	Description	Value
$\sigma = \Omega/\omega_o$	Angular speed	[0-1]
$\mu_a = M_a/M$	Lumped mass of the blade	0.245
$\mu_{\bar{a}} = m_a/M$	mass of the absorber	0.0015
$\rho_a = L_a/L$	Blade pendulum length	1
$\rho_{\bar{a}} = d_a/L$	Absorber pendulum length	0.03
$\delta = H/L$	Radius of the disk	0.72
$f_a = F_o L/K$	Strength of e.o excitation	0.04
$\xi_a = \frac{1}{L^2} \frac{C_a}{\sqrt{\frac{M}{KL^2}}}$	Blade torsional damping	0.3
$\xi_{\bar{a}} = \left(\frac{r_a}{L}\right)^2 \frac{c_a}{\sqrt{\frac{M}{KL^2}}}$	Aerodynamic damping constant	0.0002
$\xi_{\bar{a}} = \frac{1}{L^2} \frac{C_{\bar{a}}}{\sqrt{\frac{M}{KL^2}}}$	Absorber damping constant	[0-1000]
$v_a = \sqrt{K_a/K}$	Blade torsional stiffness	0.0005
$v_b = \sqrt{k_a r_a^2/K}$	Strength of the coupling between blades	0.0003
$\alpha_b$	Distance from middle of blade (point b) to the absorber base point P	0.87
$N$	Number of blades	50
$n$	Engine order excitation	6

Where the vector  $z_i = (\theta_{a_i}, \beta_{b_i})^T$  captures the sector dynamic vector and the elements of the sector mass, damping and stiffness matrices are defined below:

$$M = \begin{bmatrix} \mu_a \rho_a^2 + \mu_{\bar{a}} (\alpha_a \rho_a + \rho_{\bar{a}})^2 & \mu_{\bar{a}} \rho_{\bar{a}} (\alpha_a \rho_a + \rho_{\bar{a}}) \\ \mu_{\bar{a}} \rho_{\bar{a}} (\alpha_a \rho_a + \rho_{\bar{a}}) & \mu_{\bar{a}} \rho_{\bar{a}}^2 \end{bmatrix} \quad (10)$$

and

$$C = \begin{bmatrix} \xi_a & -\xi_{\bar{a}} \\ 0 & \xi_{\bar{a}} \end{bmatrix} \quad (11)$$

and

$$K = \begin{bmatrix} \delta \sigma^2 (\mu_a \rho_a + \mu_{\bar{a}} (\alpha_a \rho_a + \rho_{\bar{a}})) + v_a^2 & \delta \mu_{\bar{a}} \rho_{\bar{a}} \sigma^2 \\ \delta \mu_{\bar{a}} \rho_{\bar{a}} \sigma^2 & \mu_{\bar{a}} \rho_{\bar{a}} \sigma^2 (\rho_a + \delta) \end{bmatrix}. \quad (12)$$

The inter-blade coupling stiffness and damping are captured as Eq. (13):

$$K_c = \begin{bmatrix} v_b^2 & 0 \\ 0 & v_b^2 \end{bmatrix} \quad \text{and} \quad C_c = \begin{bmatrix} \xi_{\bar{a}} & 0 \\ 0 & \xi_{\bar{a}} \end{bmatrix}. \quad (13)$$

The sector force vector is given by:

$$f = \begin{bmatrix} f_a \\ 0 \end{bmatrix}. \quad (14)$$

Each  $z_i = (\theta_{a_i}, \beta_{b_i})^T$  is stacked into the configuration vector  $q = (z_1, z_2, \dots, z_N)^T$  so the governing matrix equation of motions for overall system is:

$$\hat{M}q'' + \hat{C}q' + \hat{K}q = \hat{f}e^{jn\sigma t}. \quad (15)$$

Where  $\hat{M}, \hat{C}, \hat{K}$  and  $\hat{f}$  are the overall system mass, damping, stiffness and force matrix respectively and in terms of Circulant operators, they are shown as below:

$$\left. \begin{aligned} \hat{M} &= \text{circ}(M, 0, 0, \dots, 0, 0) = \text{diag}_{i \in N}(M), \\ \hat{C} &= \text{circ}(C + 2C_c, -C_c, 0, \dots, 0, -C_c), \\ \hat{K} &= \text{circ}(K + 2K_c, -K_c, 0, \dots, 0, -K_c), \\ \hat{f} &= \text{circ}(fe^{j\phi_1}, fe^{j\phi_2}, 0, \dots, fe^{j\phi_N})^T. \end{aligned} \right\} \quad (16)$$

By exploiting the system cyclic symmetry and the Circulant structure of its matrices, the steady state forced response of the overall system can be obtained with the use of modal transformation including the complex Fourier matrix. [11, 15] Therefore Equation. (15) which is the governing matrix equation of motion for the overall  $N$ -DOF system ( $N=2$  for this investigation) is decoupled to  $N$  ( $N=2$  for this investigation) reduced-order equations. The steady-state response of a system with  $2N$  degree of freedom is converted to the solution of a single system with 2 degree of freedom under harmonic excitation. With the exception of the constant phase, which is transferred from each sector to another sector, the blades behavior is fully identical. The constant angle  $\phi_i$  shows this difference. Note that it is shown if  $n$  (engine excitation order) is an integer, the system will only be excited at mode  $n + 1$  [15].

### 3. Numerical results and discussions

In the following, elastic and linear viscoelastic behavior of the blade have been considered and compared via using parameters values, which are mentioned in Table 2. Equivalent viscoelastic parameters of the blade have been considered according to Eq. (4). First, the area under the frequency response curve of the single isolated blade without the absorber is represented in Table 3. (For this aim, parameters of the absorber are considered equal to zero)

Table 3  
The areas under the frequency response curve of the single isolated blade

$S_{VW}$ (viscoelastic blade without vibration absorber)	0.00204
$S_{EW}$ (elastic blade without vibration absorber)	0.0157

It is clear that the area under system frequency response curve for the viscoelastic blade, which is demonstrated by  $S_{VW}$ , is smaller than  $S_{EW}$  that is represented that area for elastic blade. For the viscoelastic blades, the dissipated energy reduced by 87% in relative to the elastic blades.

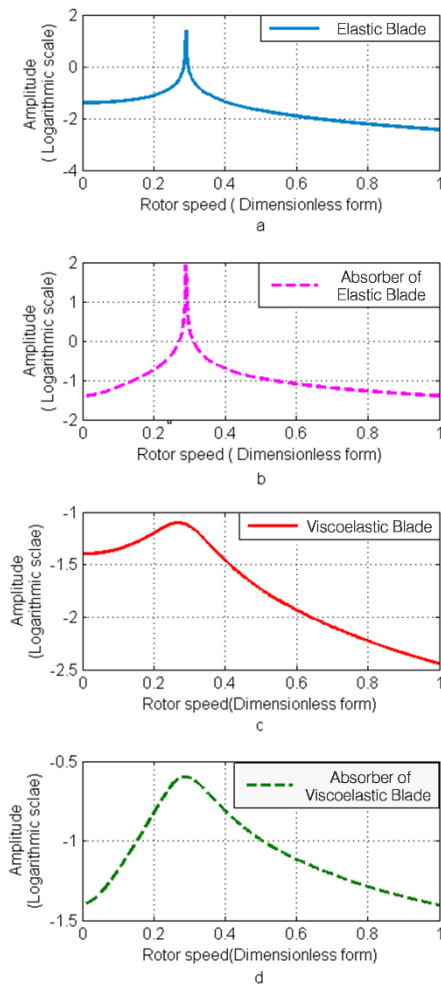


Fig. 3 Amplitude frequency response versus rotor speed (in dimensionless form) for values that are presented in Table 3: a - elastic blade, b - absorber of elastic blade, c - viscoelastic blade, d - absorber of viscoelastic blade

Design parameters include the mass, length of the pendulum of the absorber and its damping is determined optimally from the wide range of each parameters and with simultaneous use of  $H_2$  optimization criterion [19] and common numerical methods. The aim of the  $H_2$  optimization criterion is to reduce the total vibration energy of the system over all frequency. Reduction of the dissipated energy will prevent the failures like High Cycle Fatigue. Then with using of content of Table 3, the absorber is considered and amplitude of the frequency response curve of the system is illustrated in Fig. 3 as a function of rotor speed in dimensionless form. Table 4 shows the areas under the frequency response curve for Fig. 3. The viscoelastic blade can reduce dissipated energy by 89% in relative to the elastic one.

Table 4  
The areas under the system frequency response curve related to Fig. 3

$S_{VV}$ (viscoelastic blade with vibration absorber)	0.0014
$S_{EV}$ (elastic blade with vibration absorber)	0.0136

Fig. 4 shows the amplitude frequency response curve of the system with optimum values of absorber parameters for the viscoelastic and elastic blade respectively.

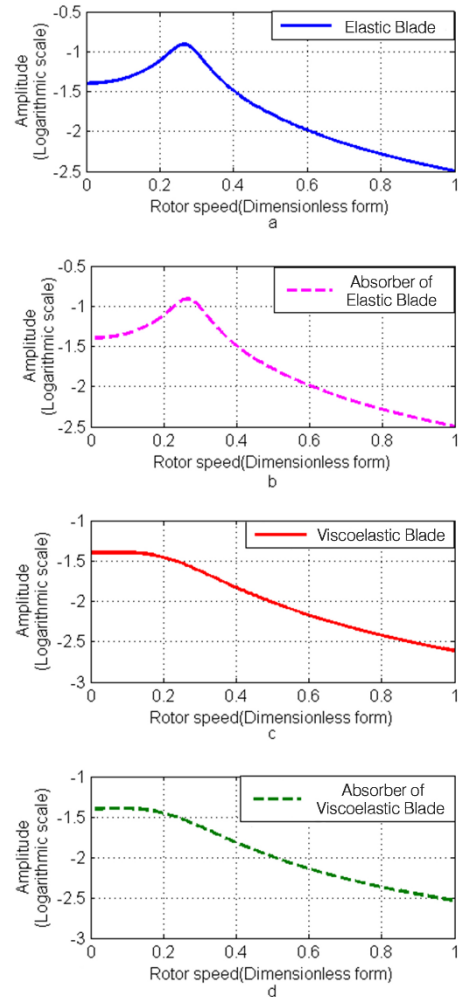


Fig. 4 Amplitude frequency response versus rotor speed (in dimensionless form) for optimum parameters: a - elastic blade, b - absorber of elastic blade, c - viscoelastic blade, d - absorber of viscoelastic blade

Tables 5 and 6 shows the area under the frequency response curve and optimum values of absorber parameters for the viscoelastic and elastic blade respectively.

Table 5

The areas under the system frequency response curve for optimum values of absorber parameters

$S_{VO}$ (viscoelastic blade with optimum vibration absorber)	0.000807
$S_{EO}$ (elastic blade with optimum vibration absorber)	0.0083

Table 6

Optimum values of the absorber parameters for the viscoelastic and the elastic blades

Value	Viscoelastic blade	Elastic blade
$\mu_{\bar{a}}$	0.00108	0.00468
$\rho_{\bar{a}}$	0.0251	0.0401
$\xi_{\bar{a}}$	0.00804	0.00461

According to Table 7, it is clear that the viscoelastic blades, even when they are not equipped with the vibration absorber, reduce dissipated energy more than the elastic blade (almost 87%) and even elastic blade which is equipped with optimum vibration absorber (almost 75%).

Table 7

Ratio of the areas that are mentioned in Tables 3 and 5

1	$S_{VW}/S_{EW}$	13%
2	$S_{VW}/S_{EO}$	25%
3	$S_{VO}/S_{VW}$	40%
4	$S_{VO}/S_{EW}$	6%
5	$S_{VO}/S_{EO}$	10%
6	$S_{EO}/S_{EW}$	52%

When the viscoelastic blades are equipped with optimum centrifugally driven order tuned vibration absorber, it is observed that the dissipated energy reduced 60%, 94% and 90% in relative to the viscoelastic blade without absorber, the elastic blade without absorber and

the elastic blade with the optimum vibration absorber respectively. It is clear that the minimum area is related to the situation where the viscoelastic blade is equipped with optimum vibration absorber (row 4). Moreover, with the comparison of row 3 and 6 of Table 7, it is concluded that, optimum vibration absorber can reduce dissipated energy in the viscoelastic blade more than the elastic blade. (Up to 12%) Also with comparison of amplitude frequency response of Figs. 3 and 4, it can be concluded that the optimum vibration absorber can cause amplitude frequency response curve of viscoelastic blade to act smoother, especially in resonant frequency, than the elastic blade. In order to investigate the effect of values of absorber parameters on the system frequency response, varied amounts should be considered. For example, Table 8 shows the effects of the variation of absorber damping of the viscoelastic blade when other parameters are constant.

Table 9 shows that situation for the elastic blades. It is shown that the area under the curve of the system frequency response is changed. With the increasing the damping of the absorber, that is, by moving towards a direction in which, the absorber be locked in relative to the blade, the area under the system frequency response curve is remained constant. With the change of each other parameters, the area under system frequency response curve is deviated from its optimum conditions. It is found that the smallest area is related to the optimum values of the absorber parameters of the viscoelastic blade.

It is important to declare that to study the characterization of the elastic blade, the effects of viscosity of the material have been ignored. Hence for elastic situation, the blade lumped damping ( $C_a$ ) and its torsional damping in dimensionless form ( $\xi_a$ ) is equal to zero in all equations.

To emphasize the results of this investigation, the study of Olson [15] is examined. He considered the undamped absorber with fixed mass and with the parameter of  $\beta$  as the absorber detuning parameter and extracted the system frequency response for different conditions. He also disregarded the effects of aerodynamic damping. Note that he had considered the elastic characterizations for both blade and disk. Definitions and values in [15] are assembled on the formulas and methods of this investigation and results are obtained and compared with results of [15] in Fig. 5. Results are matched and accuracy of this investigation is approved.

Table 8

Different values for the absorber damping while other parameters are constant (viscoelastic blade)

$\mu_{\bar{a}}$	0.00108	0.00108	0.00108	0.00108	0.00108	0.00108	0.00108
$\rho_{\bar{a}}$	0.0251	0.0251	0.0251	0.0251	0.0251	0.0251	0.0251
$\xi_{\bar{a}}$	8*e-4	8*e-3	8*e-2	8*e-1	8*e0	8*e1	8*e2
$S_P$	0.000978	0.000807	0.000912	0.00152	0.00187	0.00218	0.00218

Table 9

Different values for the absorber damping while other parameters are constant (elastic blade)

$\mu_{\bar{a}}$	0.00468	0.00468	0.00468	0.00468	0.00468	0.00468	0.00468
$\rho_{\bar{a}}$	0.0401	0.0401	0.0401	0.0401	0.0401	0.0401	0.0401
$\xi_{\bar{a}}$	4*e-4	4*e-3	4*e-2	4*e-1	4*e0	4*e1	4*e2
$S_C$	0.0112	0.0083	0.0124	0.0131	0.0152	0.0161	0.0161

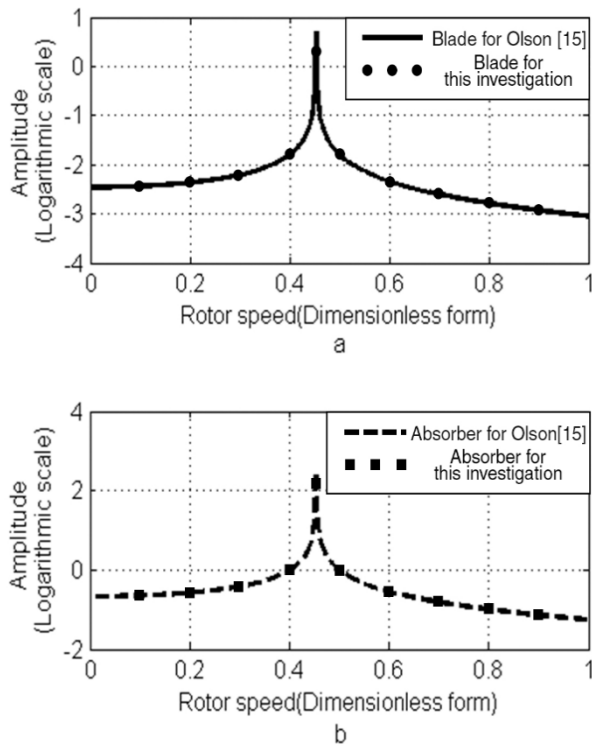


Fig. 5 Comparison of amplitude frequency response (Logarithmic scale) versus rotor speed (in dimensionless form) between Olson [15] and this investigation: a – blade, b - absorber

## 5. Conclusions

In this study, the effectiveness of the blades, which are equipped with order tuned vibration absorber for vibration suppression of the rationally periodic structures are examined. The model with one degree of freedom and equivalent parameters that represents the linear viscoelastic behavior of the blade is extracted for blades. Simple pendulum as a damped order-tuned vibration absorber is attached to the each blade and aerodynamic damping and coupling effects between the blades are considered. To attenuate vibrations during steady operation, optimized parameters of the absorber are determined. Results are compared with the behavior of the elastic blades. The main finding of this investigation is that the viscoelastic blades are more appropriate than the elastic blades to attenuate vibration especially in the resonance zone even when the elastic blades are equipped with the vibration absorber. In fact, the key recommendation of this study is to use the viscoelastic blades in the rotationally periodic structures. As was mentioned in literature, one of the various methods to reduce vibration of elastic blades is to equip them with a dynamic vibration absorber. It is clear that, design and production of the bladed disk with the dynamic vibration absorber has its own problems and in addition, as was discussed in this study before, they cannot sufficiently attenuate vibration in comparison to the viscoelastic blades. Although design and production of bladed disk with the dynamic vibration absorber has its own problems but in special cases and where smoother behavior of blades is needed and considered as a key factor, it sounds more reasonable to design these absorbers on the viscoelastic blades.

Note that the designed absorber is only capable of

removing one of the system resonances. Therefore, it seems necessary to do future works in which each blade is equipped with two or more absorbers. In this research, the absorber was moved in a circular path, so the investigation of the effects of the movement of the absorber under conditions in which it is moving in a desired way, is recommended. Although in relevant literature, some studies have been performed in which, the effects of impact absorber are investigated [19] but it seems necessary to conduct experimental studies to more accurately measure the validity of the results and to more accurately design absorber. Finally, the investigation of the effects of mistuning as an important factor in determining the behavior of the system and absorber is very important.

## References

1. **Astle, C.; Burge, I.; Chen, M.; Herrler, T.; Kwan, L.; Zibin, N.; Wood, D.** 2013. Timber for Small Wind Turbine Blades, *Energy for Sustainable Development* 17: 671-676.  
<http://dx.doi.org/10.1016/j.esd.2013.03.001>.
2. **Bhagi, L.K.; Gupta, P.; Rastogi, V.** 2013. Fractographic Investigations of the Failure of L-1 Low-Pressure Steam Turbine Blade, *Case Studies in Engineering Failure Analysis* 1, 1: 72-78.  
<http://dx.doi.org/10.1016/j.csefa.2013.04.007>.
3. **Chou, J. S.; Chiu, C. K.; Huang, I. K.; Chi, K. N.** 2013. Failure Analysis of Wind Turbine Blade Under Critical Wind Loads," *Engineering Failure Analysis*, 27: 99-118.  
<http://dx.doi.org/10.1016/j.engfailanal.2012.08.002>.
4. **Faudot, C.; Dahlhaug, O.G.** 2012. Prediction of Wave Loads on Tidal Turbine Blades," *Energy Procedia*, 20:116–133,  
<http://dx.doi.org/10.1016/j.egypro.2012.03.014>.
5. **Poursaeidi, E.; Babaei, A.; Mohammadi Arhani, M.R.; Arablu, M.** 2012. Effects of Natural Frequencies on the Failure of R1 Compressor Blades, *Engineering Failure Analysis*, 25: 304-315.  
<http://dx.doi.org/10.1016/j.engfailanal.2012.05.013>.
6. **Rao, R.; Dutta, B. K.** 2012. Vibration Analysis for Detecting Failure of Compressor Blade, *Engineering Failure Analysis*, 25: 211-218.  
<http://dx.doi.org/10.1016/j.engfailanal.2012.05.012>.
7. **Taplak, H.; Parlak, M.** 2012. Evaluation of Gas Turbine Rotor Dynamic Analysis Using the Finite Element Method, *Measurement*, 45: 1089-1097.  
<http://dx.doi.org/10.1016/j.measurement.2012.01.032>.
8. **Yang, B.** 2013. Blade Containment Evaluation of Civil Aircraft Engines, *Chinese Journal of Aeronautics*, 26: 9-16.  
<http://dx.doi.org/10.1016/j.cja.2012.12.001>.
9. **Chellil, A.; Noura, A.; Lecheba, S.; Kebirb, H.; Chevalier, Y.** 2013. Impact of the Fuselage Damping Characteristics and the Blade Rigidity on the Stability of Helicopter, *Aerospace Science and Technology*, 29: 235-252.  
<http://dx.doi.org/10.1016/j.ast.2013.03.007>.
10. **Ewins, D. J.** 1973. Vibration Characteristics of Bladed Disc Assemblies, *Journal of Mechanical Engineering Science*, 15: 165-186.  
[http://dx.doi.org/10.1243/jmes\\_jour\\_1973\\_015\\_032\\_02](http://dx.doi.org/10.1243/jmes_jour_1973_015_032_02)

11. **Gozen, S.; Olson, B.J.; Shaw, S. W.; Pierre, C.** 2012. Resonance Suppression in Multi-Dof Rotating Flexible Structures Using Order-Tuned Absorbers, *Journal of Vibration and Acoustics*, 134: 845-854. <http://dx.doi.org/10.1115/1.4007564>.
12. **Hollkamp, J.J.; Bagley, R.L.; Gordon, R.W.** 1999. A Centrifugal Pendulum Absorbers for Rotating Hollow Engine Blades, *Journal of Sound and Vibration*, 219:539-549. <http://dx.doi.org/10.1006/jsvi.1998.1964>.
13. **Kaneko, Y.; Ohta, M.; Mori, K.; Ohyama, M.** 2012. Study on Vibration Response Reduction of Bladed Disk by Use of Asymmetric Vane Spacing, *International Journal of Gas Turbine, Propulsion and Power Systems*, 4: 35-42. <http://dx.doi.org/10.1299/kikaic.78.1398>.
14. **Luo, R.** 2012. Free Transverse Vibration of Rotating Blades in a Bladed Disk Assembly, *Acta Mechanica*, 223:1385-1396. <http://dx.doi.org/10.1007/s00707-012-0655-7>.
15. **Olson, B. J.** 2006. Order-Tuned Vibration Absorbers for Systems with Cyclic Symmetry with Applications to Turbomachinery, A Dissertation for the Degree of Doctor of Philosophy, Department of Mechanical Engineering, Michigan State University, Michigan, U.S.A.
16. **Pennacchi, P.; Chatterton, S.; Bachschmid, N.; Pesatori, E.; Turozzi, G.** 2010. A Model to Study the Reduction of Turbine Blade Vibration Using the Snubbing Mechanism, *Mechanical Systems and Signal Processing*, 25: 1260-1275. <http://dx.doi.org/10.1016/j.ymssp.2010.10.006>.
17. **Shaw, S. W.; Pierre, C.** 2006. The Dynamic Response of Tuned Impact Absorbers for Rotating Flexible Structures, *Journal of Computational and Nonlinear Dynamics*, 1:13-25. <http://dx.doi.org/10.1115/1.1991872>.
18. **Asami, T.; Nishihara, O.; Baz, A. M.** 2002. Analytical Solutions to  $H_{\infty}$  and  $H_2$  Optimization of Dynamic Vibration Absorbers Attached to Damped Linear Systems, *Journal of Vibration and Acoustics*, 124: 284-295. <http://dx.doi.org/10.1115/1.1456458>.
19. **Duffy, K.P.; Bagley, R.L.; Mehmed, O.** 2000. On a Self-Tuning Impact Vibration Damper for Rotating Turbomachinery," Technical Report. National Aeronautics and Space Administration. <http://dx.doi.org/10.2514/6.2000-3100>.

Amir Abdollah Ghaderi, Alireza Mohammadzadeh, Mansour Nikkhah Bahrami

#### OPTIMUM DESIGN OF DAMPED VIBRATION ABSORBER FOR VISCOELASTIC BLADED DISK ASSEMBLIES

#### S u m m a r y

The main goal of this study is to examine the effectiveness of viscoelastic blades which are equipped with order tuned vibration absorber for vibration suppression of rationally periodic bladed disk assemblies. Kelvin-Voigt model is chosen to represent the linear viscoelastic behavior of the blade. A model with one degree of freedom is extracted for blades. Simple pendulum, as a damped order-tuned vibration absorber, is attached to the each blade. Aerodynamic damping and coupling effects between the blades are considered. A numerical method with  $H_2$  optimization criterion is used to optimize the parameters of the absorber to attenuate vibrations during steady operation. Results are compared with the behavior of the elastic blades. Finally, the literature is reviewed and validity of the results is confirmed.

**Keywords:** Viscoelastic bladed disk assemblies; Rotationally periodic structures; Order tuned vibration absorber; Damping; Optimization.

Received September 29, 2015  
Accepted November 12, 2015